Psicothema

Psicothema 2020, Vol. 32, No. 3, 337-345
doi: 10.7334/psicothema2020.92

ISSN 0214 - 9915 CODEN PSOTEG
Copyright © 2020 Psicothema
www.psicothema.com

Resting-state functional dynamic connectivity and healthy aging: A sliding-window network analysis

Núria Mancho-Fora, Marc Montalà-Flaquer, Laia Farràs-Permanyer, David Bartrés-Faz, Lídia Vaqué-Alcázar, Maribel Peró-Cebollero, and Joan Guàrdia-Olmos
University of Barcelona

Abstract

Background: Graph theory has been widely used to study structural and functional brain connectivity changes in healthy aging, and occasionally with clinical samples; in both cases, during task-related and resting-state experiments. Recent studies have focused their interest on dynamic changes during a resting-state fMRI register in order to identify differences in non-stationary patterns associated with the aging process. The objective of this study was to characterize resting-state fMRI network dynamics in order to study the healthy aging process. **Method:** 114 healthy older adults were measured in a resting-state paradigm using fMRI. A sliding-window approach to graph theory was used to measure the mean degree, average path length, clustering coefficient, and small-worldness of each subnetwork, and the impact of age and time in each graph measure was assessed. **Results:** A combined effect of age and time was detected in mean degree, average path length, and small-worldness, where participants aged 75 to 79 showed a curvilinear trend with reduced network density and increased small-world coefficient in the middle of the register. **Conclusion:** An effect of age was observed on average path length, with younger participants showing slightly lower scores.

Keywords: Dynamic functional connectivity; resting-state fMRI; sliding window correlation; healthy aging.

Resumen

Conectividad dinámica funcional en situación de reposo y envejecimiento sano: análisis de redes mediante ventanas móviles. **Antecedentes:** la Teoría de Grafos se ha utilizado para estudiar los cambios de la conectividad cerebral en el envejecimiento sano. Trabajos recientes han centrado su interés en los cambios dinámicos en registro fMRI en estado de reposo para identificar patrones no estacionarios en el proceso de envejecimiento. Este artículo tiene como objetivo caracterizar la dinámica de la red fMRI para estudiar envejecimiento saludable. **Método:** se registraron 114 adultos sanos mayores de 65 años en un paradigma de estado de reposo mediante señal fMRI. Se usó Teoría de Grafos para medir el grado medio de conectividad, la longitud promedio de las conexiones, el coeficiente de agrupamiento y el small-world de cada subred. Se evaluó el impacto de la edad y el tiempo en cada medida de grafo. **Resultados:** se detectó un efecto combinado de la edad y el tiempo en diversas medidas, los participantes de 75 a 79 años mostraron una tendencia curvilínea de la densidad y agrupación de red reducidas, pero un coeficiente small-world mayor en las ventanas centrales. **Conclusión:** se observó un efecto de la edad en la longitud promedio y los participantes más jóvenes mostraron puntuaciones más bajas en los indicadores de red.

Palabras clave: conectividad funcional dinámica; estado de reposo; *f*MRI, correlación; ventanas móviles; envejecimiento sano.

Health promotion and medical advances over recent years have had a significant impact on how long people are living. This poses major concerns about quality of life and specific pathologies affecting older adults, with particular interest in Alzheimer's Disease and other forms of dementia, which have been addressed from diverse scientific fields. Neuroscientific approaches have fixed their interest in both structural and functional brain changes measured through a wide variety of neuroimaging tools (e.g., resting-state and task-related fMRI, DTI, and volumetric MRI) modeled with a growing number of analysis techniques (Ferreira & Busatto, 2013; Sala-Llonch, Bartrés-Faz, & Junqué, 2015).

Received: March 16, 2020 • Accepted: March 30, 2020
Corresponding author: Joan Guàrdia-Olmos
Faculty of Psychology
University of Barcelona
08035 Barcelona (Spain)
e-mail: jguardia@ub.edu

Resting-state functional Magnetic Resonance Imaging (RS-fMRI) allows researchers to study hemodynamic fluctuations through blood-oxygen-level-dependent (BOLD) contrast while subjects are not performing any particular tasks. To date, one of the most common approaches in studying coactivation patterns in RS-fMRI has been through functional connectivity, where the aim is to identify synchronous hemodynamic changes in brain regions through measures derived from time-series covariance (Bastos & Schoffelen, 2016).

Recent research in aging neuroscience has described age-related differences in white matter connections and functional connectivity, even in healthy aging individuals (Damoiseaux, 2017; Geerligs, Renken, Saliasi, Maurits, & Lorist, 2014). For instance, some studies in episodic memory have detected a decrease of task-related functional connectivity in posterior brain regions coupled with an increase in posterior to frontal areas, which supports the Posterior-Anterior Shift in Aging model as well as a mechanism of compensatory scaffolding (Sala-Llonch et al., 2015). Related

to resting-state fMRI, these authors found that most studies reported a decreased connectivity between regions in the default mode network (DMN), as well as salience and attention networks. This decrease in functional connectivity and network integrity linked to the normal aging process has been found to be steeper in clinical populations such as patients with Alzheimer's Disease or Minor Cognitive Impairment (Dennis & Thompson, 2014; Farràs-Permanyer, Guàrdia-Olmos, & Peró-Cebollero, 2015).

Amongst the available analytical approaches, whole-brain functional graphs provide an insightful tool to model both healthy and dysfunctional brain network organization. In this framework, functional connectivity measures between brain regions along the fMRI register length are used as an adjacency matrix. This matrix will then help generate an undirected graph to study topological network properties such as density, modularity, centrality, clustering, or small-worldness (Bullmore & Sporns, 2009).

The effect of age on RS-fMRI network topological measures has been repeatedly investigated. Studies have found a decrease in modularity and local efficiency in the DMN (Song et al., 2014), as well as in frontoparietal control network and cingulo-opercular in networks in older participants (Geerligs et al., 2014). These authors conclude that this loss in modularity implies that networks become less specific with age. In addition to the loss of modularity, age has also been related to a decrease in the network's small-worldness (Onoda & Yamaguchi, 2013; Xu et al., 2015), which is a measure of the network's simultaneous specialization and integration. As regards functional segregation and integration, Sala-Llonch et al. (2014) found higher average path lengths and global clustering coefficients in older adults. Concerning density, Xu et al. (2015) also describe a generalized decrease in network density in older adults, in addition to a decrease in connectivity strength in temporal and occipital lobes. With this in mind, the characterization of these networks in healthy individuals allows setting a benchmark for further understanding of impaired functional structures.

In recent years, the interest has shifted from static to dynamic approaches in RS-fMRI functional connectivity. The non-stationarity of the FC measures has commonly been studied through sliding-window correlation, where a fixed time window length is defined during the fMRI scan session. Within this time window, the correlation between activity fluctuations in the areas of interest is calculated. Then the time window is shifted by a set number of data points (Hutchison et al., 2013), thus measuring the dynamic changes in FC during the RS-fMRI experiment.

Recent studies with adult populations have found that FC in intrinsic connectivity networks, such as visual and cognitive control networks, is highly non-stationary (Allen et al., 2014). Regarding graph measures in RS-fMRI, a decrease of variation has been described in network participation of FC hubs (Schaefer et al., 2014). Also, different dynamic patterns were found in clustering coefficients when comparing healthy control participants to older adults with mild cognitive impairment (Wee, Yang, Yap, & Shen, 2016b).

Although this approach has been repeatedly used in recent years, it is not exempt from notable limitations to consider. On the one hand, the non-stationary behavior of fMRI noise sources can induce changes in FC over time. For this reason, Hutchison et al. (2013) highlight the importance of hypothesis testing in the detection of changes in FC through comparisons across different populations. On the other hand, these authors also stress the difficulty in choosing adequate window lengths to balance robust estimations and the capacity to detect changes in FC. In this regard, window lengths between 30 and 60 seconds have been proposed as adequate, given that these register lengths are sufficient to correctly classify cognitive states (Shirer, Ryali, Rykhlevskaia, Menon, & Greicius, 2012).

All things considered, graph theory and dynamic functional connectivity have proven useful to understand both normal and pathological brain connectivity changes associated with the aging process. However, to our knowledge, studies combining these two approaches to connectivity analysis on older adults are still scarce. Thus, the objective of this study was to characterize resting state network dynamics in individuals with healthy aging. To that effect, we used a sliding-window approach to graph theory to measure the density, segregation, integration, and small-worldness of each subnetwork, and we assessed the impact of age and time on each graph measure.

Method

Participants

Resting-state fMRI (RS-fMRI) sequences were acquired from 114 healthy individuals (ages ranging between 48 and 89, M = 68.93, 50% females) combined from three different studies conducted at the Department of Medicine, School of Medicine and Health, University of Barcelona.

Participants were excluded if any of the following criteria were present: illiteracy, prior cerebrovascular illness, psychiatric or neurodegenerative disorders, dementia, incompatibility conditions for the MRI scanning session (such as pacemaker or other metallic objects in the body, and claustrophobia), as well as any chronic illnesses expected to shorten survival.

The original joint sample included 122 individuals. However, three individuals were excluded from the analysis due to excessive movement artifacts (root mean square movement above half a voxel), while 5 participants were excluded due to incomplete recordings.

Informed consent was obtained from each participant before the first neuropsychological screening session following the Declaration of Helsinki. Also, each of the three different protocols was approved by the institutional ethics committee. Namely, these three protocols were approved by the ethics committee of the *Comisión de Bioética de la Universidad de Barcelona* (approval number PSI2012-38257) and the ethics committee of Barcelona's *Hospital Clínic* (approval number 2009-5306 and approval number 2011-6604).

Instruments

The neuropsychological assessment aimed to attest normal cognitive functioning included Mini-Mental State Examination (Folstein, Folstein, & McHugh, 1975; Tombaugh & McIntyre, 1992), the Boston Naming Test (Kaplan, Godglass, & Weintraub, 2001), the National Adult Reading Test (Nelson, 1982), and the Vocabulary scale in the Wechsler Adult Intelligence Scale (Lezak, Howieson, & Loring, 2004). The Rey Auditory Verbal Learning Test (Rey, 1964) was applied to the participants of two protocols, while the Grober and Buschke Test (Grober & Buschke, 1987) was applied to the participants of the third protocol. These psychometric scales were administered to prevent the presence of any participants with anomalous values. None of the scores obtained indicated the presence of any types of cognitive deficit

so that no subjects were eliminated from the final sample for this reason. A more exhaustive presentation of these results can be found in Farràs et al. (2019).

Scan sessions for fMRI acquisition were preformed through a Siemens Magnetom Trio Tim syngo 3-T system at the *Centre de Diagnòstic per la Imatge* of Barcelona's *Hospital Clínic*. High-resolution T1-weighted structural image was obtained with a magnetization-prepared rapid acquisition gradient-echo (MPRAGE) 3-dimensional protocol with repetition time [TR] = 2300 ms, echo time [TE] = 2.98 ms, 240 slices, slice thickness = 1 mm, and field of view [FOV] = 256 mm.

Procedure

Resting-state fMRI sequences, with the instruction to lie down with eyes closed, was acquired in the three studies with different scan lengths:

- Protocol 1: n = 32 participants, TR = 2000 ms, TE = 16 ms, slice thickness = 3 mm, interslice gap = 25%, FOV = 220 mm, total: 5 minutes.
- Protocol 2: n = 59 participants, TR = 2000 ms, TE = 16 ms, slice thickness = 3 mm, interslice gap = 25%, FOV = 220 mm, total: 10 minutes.
- Protocol 3: n = 23 participants, TR = 2000 ms, TE = 19 ms, slice thickness = 3 mm, interslice gap = 25%, FOV = 220 mm, total: 5 minutes.

Individual RS-fMRI registers were weighted (see Data Analysis) to account for the difference in register lengths across studies.

Data analysis

The structural image data were analyzed using an FSL (FMRIB Software Library v5.0) preprocessing pipeline adapted under the authorization of Diez et al. (2015). T1 images were reoriented, and a resampled anterior and posterior commissure (ACPC) aligned image with 6 degrees of freedom (DOF) was created. Non-brain tissue was removed to obtain an anatomic brain mask to parcel and segment the T1 data images. Structural images were registered to the normalized space by using the Montreal Neurological Institute standard brain coordinates (Ashburner & Friston, 1999).

For RS-fMRI registers, thirty contiguous slices in the ACPC plane were obtained through a slice time correction based on the TR. Images were reoriented to match the template axes and motion correction was computed to co-register all the volumes with the central one. All non-brain tissue was removed, and the volumes were smoothed with a 6-mm FWHM isotropic Gaussian kernel to improve the signal-to-noise ratio. Intensity correction and bandpass filtering between 0.01 and 0.08 Hz were applied to the data. The resulting functional data images were registered and normalized to the standard MNI space. Finally, the white matter and the cerebrospinal fluid effects were removed. Also, movement artifacts were measured through Framewise Displacement and the Jenkinson's Framewise Displacement (Power, Barnes, Snyder, Schlaggar, & Petersen, 2012).

The regions of interest (ROI) were obtained through the Automatic Anatomical Labeling (AAL) atlas (Tzourio-Mazoyer et al., 2002), which defines 90 cortical and subcortical areas, where the 45 areas in each hemisphere are alternatively interspersed. Time series of all the voxels in an AAL brain area were averaged to obtain the signal of each ROI.

Due to differences in the length of the scanning sessions across protocols, only the first 150 volumes of each subject were analyzed, as done in earlier papers (Allen et al., 2014).

For each individual, their preprocessed AAL ROI RS-fMRI fluctuations were decomposed into overlapping sliding windows with a length of 30 time-points and a time-step of 10 time-points. The selection of the amplitude of the mobile window was based on some previous studies of non-dynamic functional connectivity (Farràs et al., 2018). Those studies indicated enough variability in 30 seconds and, therefore, in short-duration windows. It is known that most studies show mobile windows between 30 and 60 seconds (Zalesky & Breakspear, 2015). In each sliding-window sub-series, Pearson's correlation was calculated, thresholded with $r^2 \geq 0.5$, and binarized to obtain an adjacency matrix. This criterion was applied because it is the minimum correlation value from which the size of the effect is sufficiently high to assume a clearly significant relationship intensity according to the criteria of Xu et al. (2015). In some recent studies, the use of a low pass filter has been proposed, using the inverse of the window amplitude as the upper limit (Leonardi & Van De Ville, 2015; Rubinov & Sporns, 2010). In our case, the application of this type of criterion involved an excessive loss of variability. Therefore, we opted for a more favourable criterion of significance.

Each sliding-window network was characterized by its mean degree (MD), characteristic path length (APL), clustering coefficient (CC), and small-world coefficient (SW).

The degree refers to the total number of edges of a network, or the unique nonzero values of the adjacency matrix, and reflects the importance of each node in the network (Rubinov & Sporns, 2010). Thus, the mean degree of a network was used to inform on the density of connections in the network. The characteristic path length, or average path length, is the average shortest path length between all the possible pairs of nodes in a network and has been a standard measure of functional network integration. The clustering coefficient of a network was estimated through transitivity, i.e. the probability that any two nodes connected to a third node are also connected to themselves (Fornito, Zalesky, & Bullmore, 2016). Transitivity informs on the functional segregation of the network, expressed as the clustered connectivity around nodes.

The mean degree, characteristic path length, clustering coefficient, and small-world coefficient were estimated through the R package '*igraph*' (Csárdi & Nepusz, 2006), while the sliding-window analysis was performed with the R package '*zoo*' (Zeileis & Grothendieck, 2005).

The participants were split into six age groups (< 60, 60 to 64, 65 to 69, 70 to 74, 75 to 79, and ≥ 80) with sizes 12, 21, 29, 22, 21, and 9 respectively, in order to study differences in functional connectivity patterns. This categorization had been used in previous studies and is coherent with the suggestion made by Sala-Llonch, Bartrés, and Junqué (2015). Moreover, the age effect on the time series of the graph descriptive measures was estimated through repeated measures ANOVA.

Results

Table 1 summarizes the sample distribution of each graph measure (MD, APL, CC, and SW) for each age group. Figure

number 1 shows the observed static distribution of each index point during the time of the register. We have incorporated the boxplots to explain the variability in each point of the serial registers, represented in the box distance ($Q_1 - Q_3$).

Table 1
Descriptive statistics of the static mean degree, average path length, cluster coefficient, and small-world for each group

Measure	Age	Mean	SD	Skewness	Kurtosis
Mean Degree	<60	23.080	9.293	0.499	2.133
	60-64	17.691	6.071	0.504	2.454
	65-69	18.558	9.559	1.237	4.312
	70-74	20.834	8.442	0.954	2.972
	75-79	15.089	4.705	-0.138	1.981
	80+	19.156	5.866	0.037	1.316
Average Path Length	<60	2.178	0.355	0.745	2.639
	60-64	2.367	0.309	0.286	2.246
	65-69	2.458	0.437	-0.246	2.447
	70-74	2.292	0.339	-0.177	1.844
	75-79	2.497	0.324	0.491	2.279
	80+	2.277	0.267	0.210	1.433
Clustering Coefficient	<60	0.636	0.095	0.781	2.867
	60-64	0.605	0.081	-0.147	1.791
	65-69	0.625	0.093	-0.094	2.044
	70-74	0.637	0.090	0.738	2.792
	75-79	0.595	0.097	-0.755	3.817
	80+	0.629	0.058	-0.012	1.415
Small World	<60	2.275	0.608	0.842	2.626
	60-64	2.679	0.603	0.795	3.042
	65-69	2.791	0.841	0.329	2.035
	70-74	2.420	0.504	0.053	1.801
	75-79	3.029	0.652	0.307	2.041
	80+	2.580	0.573	0.438	1.736

According to the observed distributions of the different variables, we carried out a univariate analysis of repeated measures using each index, following a mixed structure deriving from age groups and time series points. Additionally, the homogeneity Box test suggested that the observed covariance matrices of the graph measures were homoscedastic distributions across the groups and time series for APL ($F_{(273,\ 15083.127)} = 0.985$, p = 0.556); CC ($F_{(273,\ 15083.127)} = 1.022$, p = 0.389) and SW ($F_{(273,\ 15083.127)} = 1.121$, p = 0.085), and not homoscedastic for the mean degree ($F_{(273,\ 15083.127)} = 1.334$, p < 0.001). Moreover, Mauchly's test indicated that the assumption of sphericity was not accepted in all graph measures ($p < .001$), which justifies the use of multivariate estimations with estimations based on Greenhouse-Geisser correction to avoid these effects (see table number 2 and table number 3).

As *a posteriori* analysis, as shown in table 2, quadratic models for age effect were significant for all measures, which suggests relevant nonlinear trends across time points (MD with $p = .02$; APL with $p = .024$; CC with $p = .021$ and SW with $p = .003$)

Significant but weak age effect with low intensity was detected on mean degree ($F_{(5,\ 108)} = 2.697$; p = 0.024; $\varepsilon^2 = 0.111$), as well as an interaction of age and time with poor intensity ($F_{(28.939,\ 625.090)} = 1.508$; p = 0.044; $\varepsilon^2 = 0.065$), which points towards differential trends across age groups. More specifically, participants aged 75 to 79 showed a decreased mean degree in the middle of the scanning session, while participants aged below 60 showed an opposite trend (Figure 2). Additionally, participants aged 65 to 69 showed a slightly increasing trend in mean degree during the registered scanning session, while participants aged 70 to 74 showed a slightly decreasing trend.

As regards average path length, the effect of age was significant but weak ($F_{(5,\ 108)} = 2.781$; p = 0.021; $\varepsilon^2 = 0.114$), with younger participants showing networks with a slightly lower average path length (Figure 3), which suggests a higher network integration

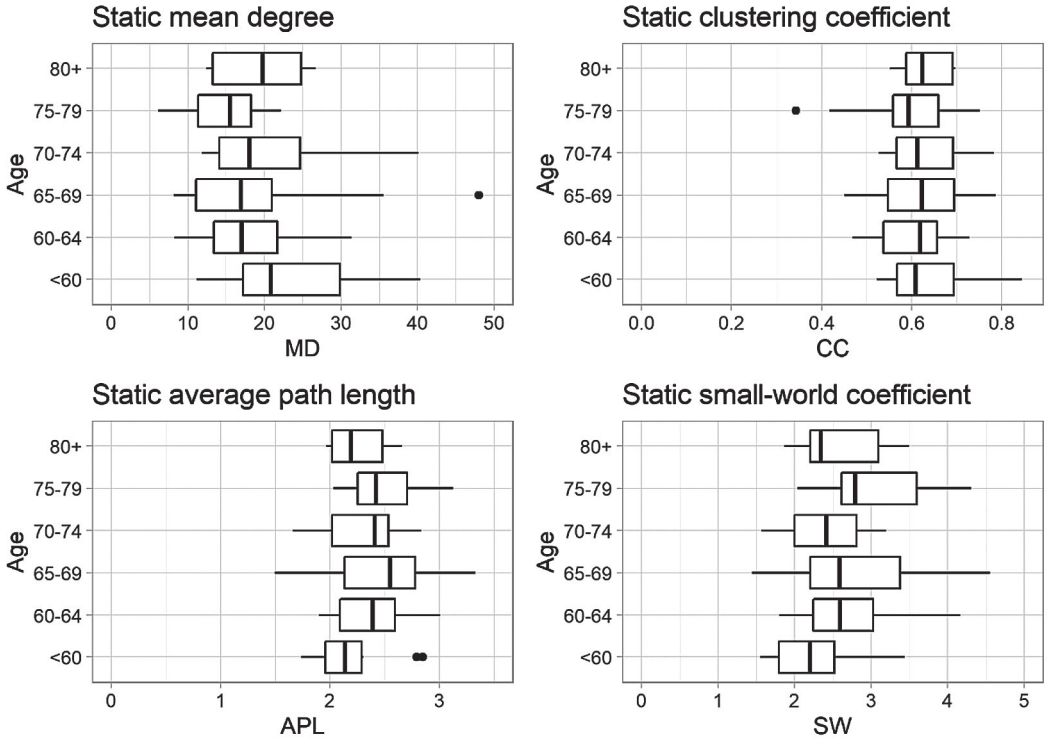

Figure 1. Observed distribution for each static index according to the age group

Table 2
Multivariate analysis of repeated measures for each graph measure (I)

	Mean Degree					Average Path Length				
Source	**F**	**df**	**p**	**ε²**	**1-β**	**F**	**df**	**p**	**ε²**	**1-β**
Time	.725	5.788; 625.090	.625	.007	.284	.564	5.639; 608.977	.748	.005	.221
Age	2.697	5; 108	.025	.111	.800	2.781	5; 108	.021	.114	.813
Time*Age	1.508	28.939; 625.090	.044	.065	.983	1.774	28.193; 608.977	.009	.076	.994
QM			.020					.024		

QM: Best quadratic model; F: empiric Fisher F statistic; *p*: p-value associated to *F* statistic; ε^2: effect size; *1-β*: power estimation

Table 3
Multivariate analysis of repeated measures for each graph measure (II)

	Clustering Coefficient					Small World				
Source	**F**	**df**	**p**	**ε²**	**1-β**	**F**	**df**	**p**	**ε²**	**1-β**
Time	.798	7.755; 837.491	.601	.007	.370	.995	6.509; 702.947	.431	.009	.416
Age	1.284	5; 108	.276	.056	.440	2.637	5; 108	.027	.109	.789
Time*Age	.871	38.773; 837.491	.695	.039	.890	1.840	32.544; 702.947	.003	.078	.998
QM			.021					.003		

QM: Best quadratic model; F: empiric Fisher F statistic; *p*: p-value associated to *F* statistic; ε^2: effect size; *1-β*: power estimation

potential. No significant intra-series effects were detected. We also detected a significant but weak interaction effect between age and time for average path length ($F_{(28.193,\ 608.977)} = 1.774$; $p = 0.009$; $\varepsilon^2 = 0.076$)

We found no statistically significant effects of age or time on the clustering coefficients in our participants. However, participants aged 60 to 64 presented slightly lower values at the end of the series, while participants aged 70 to 74 showed higher values in the middle of the registered session (Figure 4). Participants aged under 60, as well as the older group, showed higher variability during the scanning session compared to the other groups.

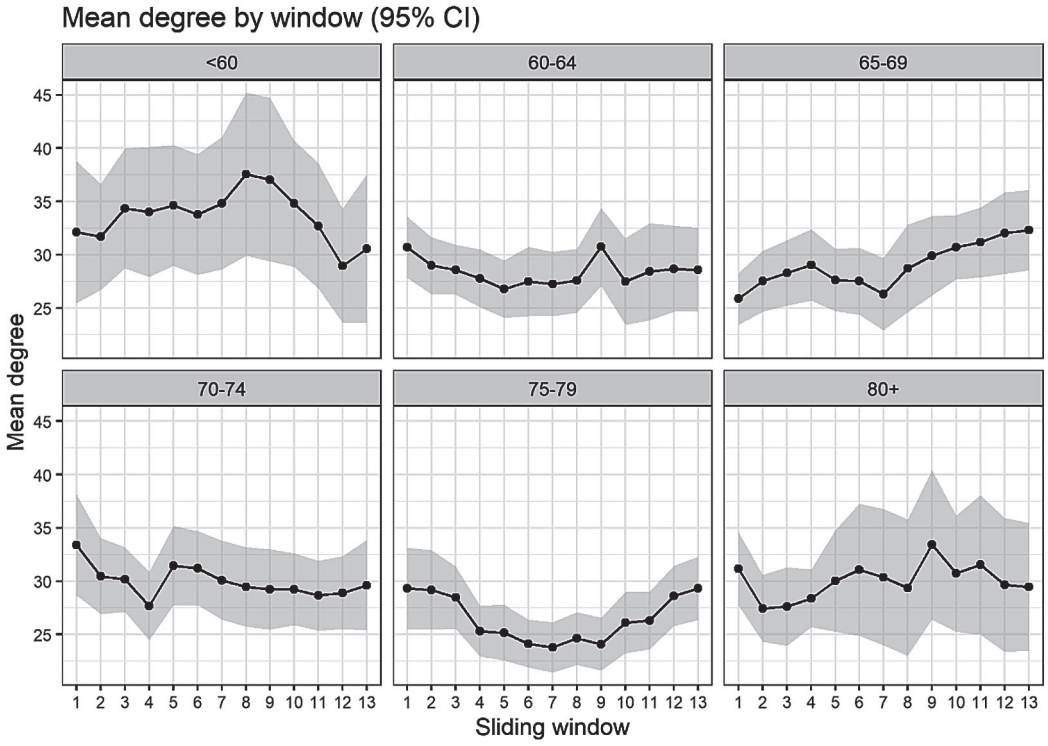

Figure 2. Mean degree path length of the networks by sliding window

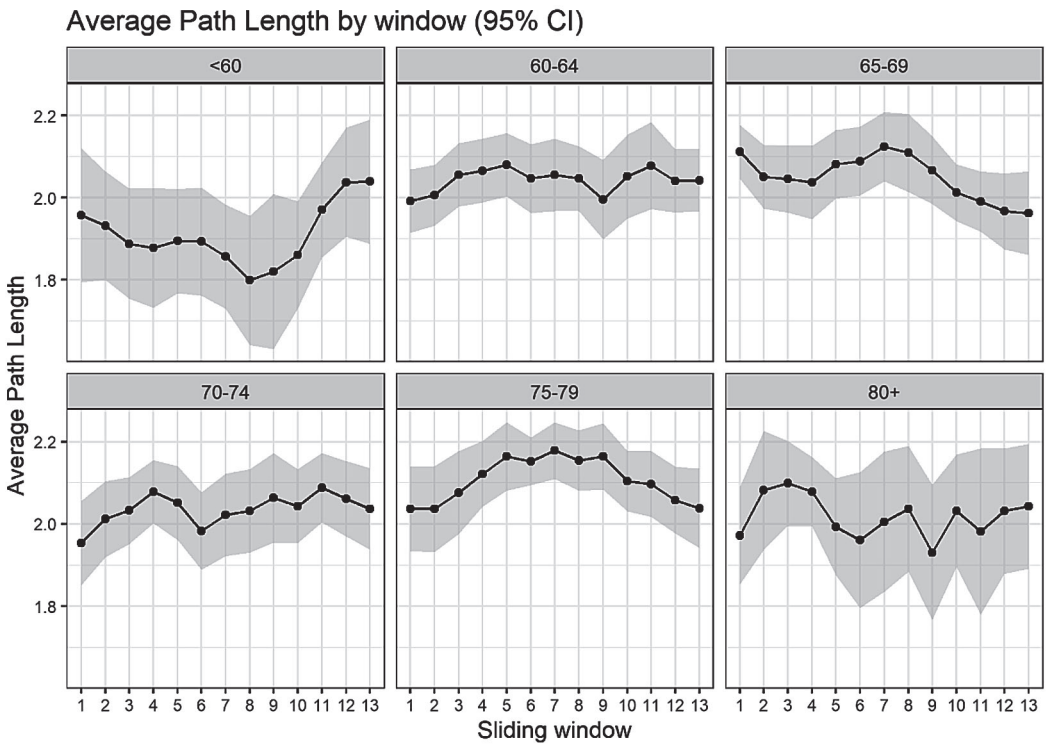

Figure 3. Average path length of the networks by sliding window

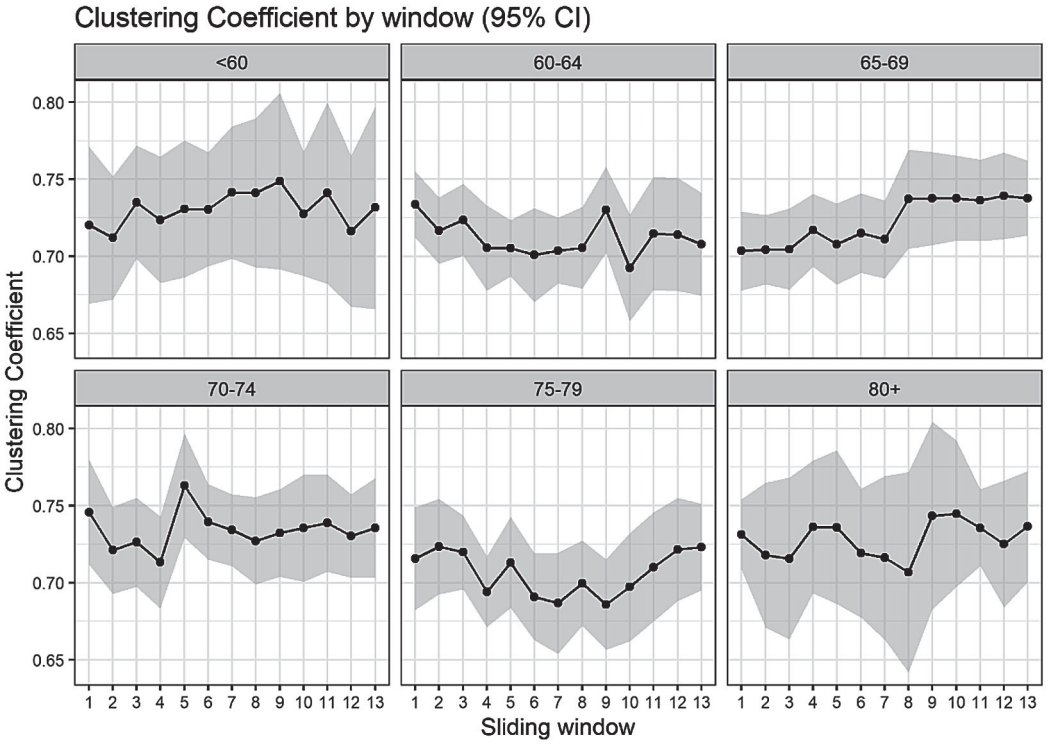

Figure 4. Average clustering coefficient of the networks by sliding window

Finally, regarding the small-world coefficient, significant but weak effects of age were detected ($F_{(5, 108)}$ = 2.637; p = 0.027; ε^2 = 0.109), as well as an interaction between age and time ($F_{(32.544, 702.947)}$ = 1.840; p = 0.003; ε^2 = 0.078). Participants aged 75 to 79 showed higher values in the middle of the registered series while participants' ages below 60 showed an opposed trend (Figure 5). In

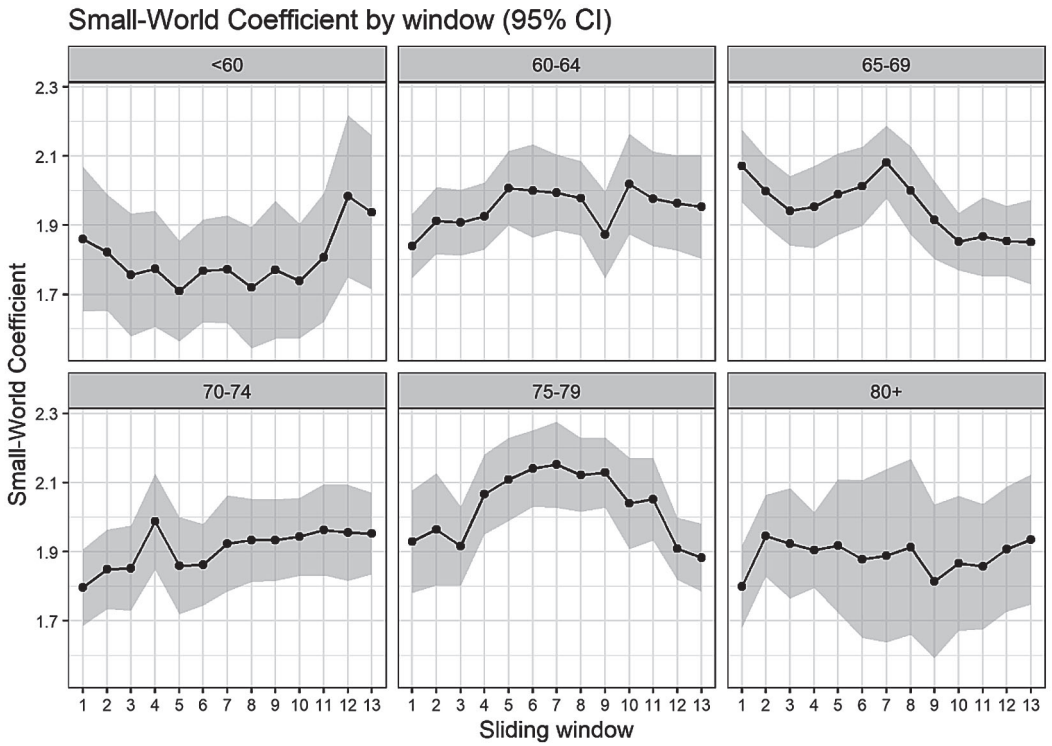

Figure 5. Average small-world coefficient of the networks by sliding window

addition, participants aged 65 to 69 presented a decreasing trend, while those aged 70 to 74 showed a slightly increasing trend.

Discussion

In this study, we aimed to characterize RS-fMRI network dynamics in healthy older adults through a sliding-window approach to graph theory. ROI time series were segmented into 13 overlapping windows, where Pearson's correlation matrices were calculated. These correlation matrices were thresholded and binarized to obtain a graph adjacency matrix where the mean degree, average path length, clustering coefficient, and small-world coefficient were studied. The effect of the age group and the time dynamics were assessed for each graph measure.

This study highlighted an effect of age and window on the mean degree, as opposing trends were detected between participants aged 75 to 79 and those aged under 60, the former showing a decrease in network degree halfway through the register. This age effect falls in line with the generalized loss in network density in older adults previously attested (Xu et al., 2015).

Significant but weak effects of the time window were detected in the average path length, with the younger group showing lower values, which suggests a highly integrated functional network. In addition, participants aged 70 to 74 showed higher scores in clustering coefficient in the middle of the scanning session. These findings are coherent with the higher average path length and global clustering coefficient in older adults (Sala-Llonch et al., 2014).

Finally, we detected significant age and window effects on the small-world coefficient. More specifically, participants aged 75 to 79 showed generally higher values in the small-world coefficient as well as a quadratic trend during the register length. Thus, our study does not clearly confirm the loss in small-worldness in older individuals found by previous studies (Onoda & Yamaguchi, 2013; Xu et al., 2015). Our interpretation of this discrepancy focuses on the fact that our sample comprises older subjects than the samples of the cited papers. That implies that we have healthy older individuals and, therefore, they do not show cognitive impairment. The complexity indicators of the networks studied remain more stable than those described by those previous studies.

In addition to all of the above, this paper reveals a significant new contribution. It presents the generation of an analysis framework that combines the approximation through graphs to the behavior of dynamic connectivity series with classical techniques. This issue is especially relevant since we understand that our results compel us to consider complex connectivity systems as non-static systems with elements that can be modified in their structure and functionality over the recorded period. If we can find the variability presented in this study in relatively short times, it is reasonable to think that, in longer series, the results will even be much more complex. Likewise, consideration should be given to the generation of other connectivity indicators to further establish the properties and statistical behavior of the detected networks (Adhikari et al., 2017).

Several limitations of this study should be considered. To begin with, both the younger and older groups comprised fewer individuals and revealed higher variability in all the dynamic graph estimates. That hinders comparability with the other age groups. Higher variability in the older group could also be explained by a survival bias of these participants. More specifically, those individuals who live up to this age and score above the neuropsychological criteria might have better preserved FC networks.

As regards methodological limitations, it should be noted that methods based on product-moment correlation assume independence of the observations, which should not be expected in time-series data. However, we opted for this analysis as an FC measure, given the simplicity of the estimator and previous work in the field. Moreover, it is important to bear in mind some limitations of the correlation estimation due to the difficulty in separating the effects of the interactions (Smith et al., 2011) or the variation generated by the stochastic noise (Handwerker, González-Castillo, D'Esposito, & Bandettini, 2012; Hutchison et al., 2013).

Finally, to identify new research lines derived from the dynamic estimation of connectivity, we consider it might be interesting to take the following steps: i) comparing healthy and impaired populations; ii) analyzing the effects of neuropsychological tests on network measures; and iii) working with undirected, weighted networks.

Acknowledgements

This study was supported by the *Grup of Quantitative Psychology*, members of the *Generalitat de Catalunya*'s SGR 266 Consolidated Research Group (GRC), and it was made possible by the PSI2013-41400-P project of the Spanish Government's *Ministerio de Economía y Competitividad*.

References

Adhikari, M. H., Hacker, C. D., Siegel, J. S., Griffa, A., Hagmann, P., Deco, G., & Corbetta, M. (2017). Decreased integration and information capacity in stroke measured by whole brain models of resting state activity. *Brain*, *140*(4), 1068-1085. doi:10.1093/brain/awx021

Allen, E. A., Damaraju, E., Plis, S. M., Erhardt, E. B., Eichele, T., & Calhoun, V. D. (2014). Tracking whole-brain connectivity dynamics in the resting state. *Cerebral Cortex*, *24*(3), 663-676. doi:10.1093/cercor/bhs352

Ashburner, J., & Friston, K. J. (1999). Nonlinear spatial normalization using basis functions. *Human Brain Mapping*, *7*(4), 254-266. doi: 10.1002/(SICI)1097-0193

Bastos, A. M., & Schoffelen, J.-M. (2016). A tutorial review of functional connectivity analysis methods and their interpretational Pitfalls. *Frontiers in Systems Neuroscience*, *9*, 175. doi:10.3389/fnsys.2015.00175

Bullmore, E., & Sporns, O. (2009). Complex brain networks: Graph theoretical analysis of structural and functional systems. *Nature Neuroscience*, *10*(3), 186-198. doi:10.1038/nrn2575

Csárdi, G., & Nepusz, T. (2006). The igraph software package for complex network research. *International Journal of Complex Systems*, *1695*(5), 1-9.

Damoiseaux, J. S. (2017). Effects of aging on functional and structural brain connectivity. *NeuroImage, 160*, 32-40. doi:10.1016/j.neuroimage.2017.01.077

Ferreira, L. K., & Busatto, G. F. (2013). Resting-state functional connectivity in normal brain aging. *Neuroscience and Biobehavioral Reviews, 37*(3), 384-400. doi:10.1016/j.neubiorev.2013.01.017

Farras, L., Mancho, N., Montalà, M., Bartrés, D., Vaqué, L., Peró, M., & Guardia, J.. (2019). Age-related decrease in resting-state functional connectivity in older groups. *Neural Regeneration Research*, *14*(9), 1544-1555. doi:10.4103/1673-5374.255976

Folstein, M. F., Folstein, S. E., & McHugh, P. R. (1975). "Mini-mental state". A practical method for grading the cognitive state of patients for the clinician. *Journal of Psychiatric Research*, *12*(3), 189-198. doi:10.1016/0022-3956(75)90026-6

Fornito, A., Zalesky, A., & Bullmore, E. (2016). Fundamentals of brain network analysis. *Fundamentals of Brain Network Analysis*. London: Academic Press.

Geerligs, L., Renken, R. J., Saliasi, E., Maurits, N. M., & Lorist, M. M. (2014). A Brain-Wide study of age-related changes in functional connectivity. *Cerebral Cortex*, *25*(7), 1987-1999. doi:10.1093/cercor/bhu012

Grober, E., & Buschke, H. (1987). Genuine memory deficits in dementia. *Developmental Neuropsychology*, *3*(1), 13-36. doi:10.1080/87565648709540361

Handwerker, D. A., González-Castillo, J., D'Esposito, M., & Bandettini, P. A. (2012). The continuing challenge of understanding and modeling hemodynamic variation in fMRI. *NeuroImage*, *62*(2), 1017-1023. doi:10.1016/j.neuroimage.2012.02.015

Hutchison, R. M., Womelsdorf, T., Allen, E. A., Bandettini, P. A., Calhoun, V. D., Corbetta, M., … Chang, C. (2013). Dynamic functional connectivity: Promise, issues, and interpretations. *NeuroImage*, *80*, 360-378. doi:10.1016/j.neuroimage.2013.05.079

Kaplan, E., Godglass, H., & Weintraub, S. (2001). *Boston naming test*. Austin: PRO-ED.

Lezak, M. D., Howieson, D. B., & Loring, D. W. (2004). *Neuropsychological Assessment*. New York: Oxford University Press.

Leonardi, N., & Van De Ville, D. (2015). On spurious and real fluctuations of dynamic functional connectivity during rest. *Neuroimage*, *104*, 430-436.

Nelson, H. E. (1982). *The National Adult Reading Test (NART): Test manual*. Windsor: NFER Nelson.

Onoda, K., & Yamaguchi, S. (2013). Small-worldness and modularity of the resting-state functional brain network decrease with aging. *Neuroscience Letters*, *556*, 104-108. doi:10.1016/j.neulet.2013.10.023

Power, J. D., Barnes, K. A., Snyder, A. Z., Schlaggar, B. L., & Petersen, S. E. (2012). Spurious but systematic correlations in functional connectivity MRI networks arise from subject motion. *NeuroImage*, *59*(3), 2142-2154. doi:10.1016/j.neuroimage.2011.10.018

Rey, A. (1964). *Clinical tests in psychology*. Paris: Presses Universitaires de France.

Rubinov, M., & Sporns, O. (2010). Complex network measures of brain connectivity: Uses and interpretations. *NeuroImage*, *52*(3), 1059-1069. doi:10.1016/j.neuroimage.2009.10.003

Sala-Llonch, R., Bartrés-Faz, D., & Junqué, C. (2015). Reorganization of brain networks in aging: A review of functional connectivity studies. *Frontiers in Psychology*, *6*. doi:10.3389/fpsyg.2015.00663

Sala-Llonch, R., Junqué, C., Arenaza-Urquijo, E. M., Vidal-Piñeiro, D., Valls-Pedret, C., Palacios, E. M., … Bartrés-Faz, D. (2014). Changes in whole-brain functional networks and memory performance in aging. *Neurobiology of Aging*, *35*(10), 2193-2202. doi:10.1016/j.neurobiolaging.2014.04.007

Schaefer, A., Margulies, D. S., Lohmann, G., Gorgolewski, K. J., Smallwood, J., Kiebel, S. J., … Von, C. (2014). Dynamic network participation of functional connectivity hubs assessed by resting-state fMRI. *Frontiers in Human Neuroscience*, *8*, 195. doi:10.3389/fnhum.2014.00195

Shirer, W. R., Ryali, S., Rykhlevskaia, E., Menon, V., & Greicius, M. D. (2012). Decoding Subject-Driven Cognitive States with Whole-Brain Connectivity Patterns. *Cerebral Cortex*, *22*(1), 158-165. doi:10.1093/cercor/bhr099

Smith, S. M., Miller, K. L., Salimi-Khorshidi, G., Webster, M., Beckmann, C. F., Nichols, T. E., … Woolrich, M. W. (2011). Network modelling methods for FMRI. *NeuroImage*, *54*(2), 875-891. doi:10.1016/j.neuroimage.2010.08.063

Song, J., Birn, R. M., Boly, M., Meier, T. B., Nair, V. A., Meyerand, M. E., & Prabhakaran, V. (2014). Age-Related Reorganizational Changes in Modularity and Functional Connectivity of Human Brain Networks. *Brain Connectivity*, *4*(9), 662-676. doi:10.1089/brain.2014.0286

Tombaugh, T. N., & McIntyre, N. J. (1992). The mini-mental state examination: A comprehensive review. *Journal of the American*

Geriatrics Society, 40(9), 922-935. doi:10.1111/j.1532-5415.1992.tb01992.x

Tzourio-Mazoyer, N., Landeau, B., Papathanassiou, D., Crivello, F., Etard, O., Delcroix, N., … Joliot, M. (2002). Automated Anatomical Labeling of Activations in SPM Using a Macroscopic Anatomical Parcellation of the MNI MRI Single-Subject Brain. *NeuroImage*, *15*(1), 273-289. doi:10.1006/nimg.2001.0978

Wee, C.-Y., Yang, S., Yap, P.-T., & Shen, D. (2016a). Sparse temporally dynamic resting-state functional connectivity networks for early MCI identification. *Brain Imaging and Behavior*, *10*(2), 342-356. doi:10.1007/s11682-015-9408-2

Wee, C.-Y., Yang, S., Yap, P.-T., & Shen, D. (2016b). Sparse temporally dynamic resting-state functional connectivity networks for early MCI identification for the Alzheimer's Disease Neuroimaging Initiative. *Brain Imaging and Behavior*, *10*, 342-356. doi:10.1007/s11682-015-9408-2

Xu, X., Kuang, Q., Zhang, Y., Wang, H., Wen, Z., & Li, M. (2015). Age-related changes in functional connectivity between young adulthood and late adulthood. *Analytical Methods*, *7*(10), 4111-4122. doi:10.1039/C5AY00699F

Zalesky, A., & Breakspear, M. (2015). Towards a statistical test for functional connectivity dynamics. *Neuroimage*, *114*, 466-470. doi:10.1016/j.neuroimage.2015.03.047

Zeileis, A., & Grothendieck, G. (2005). Infrastructure for Regular and Irregular Time Series. *Journal of Statistical Software*, *14*(6). doi:10.18637/jss.v014.i06